Stanford Exploration Project, Report 110, September 18, 2001, pages 1–18

Amplitude preserving prestack imaging of irregularly sampled 3-D data

Biondo Biondi and Ioan Vlad[1]

ABSTRACT

We introduce a computationally efficient and robust method to regularize acquisition geometries of 3-D prestack seismic data before prestack migration. The proposed method is based on a formulation of the geometry regularization problem as a regularized least-squares problem. The model space of this least-squares problem is composed of uniformly sampled common offset-azimuth cubes. The regularization term fills the acquisition gaps by minimizing inconsistencies between cubes with similar offset and azimuth. To preserve the resolution of dipping events in the final image, the regularization term includes a transformation by Azimuth Moveout (AMO) of the common offset-azimuth cubes. The method is computationally efficient because we applied the AMO operator in the Fourier-domain, and we precondition the least-squares problem. Therefore, no iterative solution is needed and excellent results are obtained by applying the adjoint operator followed by a diagonal weighting in the model domain.

We tested the method on a 3-D land data set from South America. Subtle reflectivity features are better preserved after migration when the proposed method is employed as compared to more standard geometry regularization methods. Furthermore, a dipping event at the reservoir depth (more than 3 km) is better imaged using the AMO regularization as compared to a regularization operator that simply smoothes the data over offsets.

INTRODUCTION

Irregular acquisition geometries are a serious impediment to the accurate imaging of the subsurface. When the data are irregularly sampled, images are often affected by amplitude artifacts and phase distortions, even if the imaging algorithm employed is designed to preserve amplitudes. Addressing this problem becomes more crucial when the goal is to use information contained in the image amplitudes. In these cases, the application of a simple imaging sequence that relies on standard 'adjoint' imaging operators is likely to produce misleading results. Amplitude-preserving imaging of irregular geometries is thus one area of seismic processing that can greatly benefit from the application of inverse theory, and extensive research have been carried out in this direction.

There are two distinct approaches that can be used to apply inverse theory to the prob-

[1]**email:** biondo@sep.stanford.edu

lem. The first one attempts to regularize the data geometry before migration (Duijndam et al., 2000), while the second one attempts to correct for the irregular geometries during migration (Albertin et al., 1999; Bloor et al., 1999; Audebert, 2000; Rousseau et al., 2000; Duquet et al., 1998; Nemeth et al., 1999). The main strength of the latter approach is also its main weakness; it is model based; in particular, it depends on an accurate knowledge of the interval velocity model. If the model is well known, the methods based on the inversion of imaging operators have the potential of being accurate, because they exploit the intrinsic correlation between seismic traces recorded at different locations. However, when the uncertainties on the model are large, these methods can be also unreliable. Furthermore, a full prestack migration is an expensive process. Its substitution with an inversion process, even if iterative or approximate, might be beyond the practical reach.

In this paper we propose a method that has the advantages of both approaches. We regularize the data geometry before migration, but to fill the acquisition gaps we use a partial migration operator that exploits the intrinsic correlation between prestack seismic traces. The imaging operator is Azimuth Moveout (AMO) (Biondi et al., 1998), that depends on a priory knowledge of RMS velocity. RMS velocity can be estimated from the data much more robustly than interval velocity.

Ronen (1987) was the first to use a partial migration operator to improve the estimate of a regularized data set. His method uses dip moveout (DMO) to regularize stacked cubes. Chemingui and Biondi (1997; 1999) have previously inverted AMO to create regularly sampled common offset-azimuth cubes. The main advantages of the method proposed in this paper over the previous methods are: a) it is based on a Fourier-domain implementation of AMO (Vlad and Biondi, 2001), as opposed to a Kirchhoff implementation, and thus it is computationally efficient and its implementation is straightforward, b) it uses AMO in the regularization equation (model styling) formulation of a regularized least-squares inverse problem, instead that in the modeling equation. In this formulation, the regularization term can be effectively preconditioned, with a substantial gain in computational efficiency, c) it approximates the solution of the preconditioned least-squares problem by applying normalization weights to the model vector after the application of the adjoint operator. Therefore, it avoids the costs and pitfalls of iterative solutions.

Our formulation of the geometry regularization problem as a regularized least-squares problem is similar to the formulation that Fomel presented in his Ph.D. thesis (2001). He uses a finite difference implementation of offset continuation where we use a Fourier implementation of AMO. These two operators are kinematically equivalent, and their computational efficiency is similar. However, the methods are different with respect to items b) and c) listed above. Our method should be more efficient because it explicitly preconditions the regularization term by inverting it. The inversion is fast because exploits the fact that the regularization matrix can be factored into the product of a block lower-diagonal matrix with a block upper-diagonal matrix, which are easily invertible by recursion. The preconditioning substantially improves the conditioning of the problem; therefore, a simple diagonal normalization of the model vector yields a good and fast solution to the problem.

NORMALIZED PARTIAL STACKING AND INVERSE THEORY

Our goal is to create uniformly sampled common offset/azimuth cubes, that can be migrated using an amplitude-preserving algorithm. The main tool to create these common offset/azimuth cubes is partial stacking the data recorded with irregular geometries within offset and azimuth ranges.

Stacking is the operation of averaging seismic traces by summation. It is an effective way to reduce the size of data sets and to enhance reflections while attenuating noise. To avoid attenuating the signal together with the noise, the reflections need to be coherent among the traces that are being stacked. A common method to increase trace coherency is to apply Normal Moveout (NMO). NMO is a first-order correction for the differences in timings among the reflections in traces recorded at different offsets. Global stacking of all the traces recorded at the same midpoint location, no matter their offset and azimuth, is the most common type of stacking. Partial stacking averages only those traces with offset and azimuth within a given range.

The first problem that we encounter when stacking 3-D prestack data is that, because of acquisition geometry irregularities, data traces do not share the same exact midpoint location. Stacking 3-D prestack data is thus the combination of two processes: spatial interpolation followed by averaging. To start our analysis we define a simple linear model that links the recorded traces (at arbitrary midpoint locations) to the stacked volume (defined on a regular grid). Each data trace is the result of interpolating the stacked traces, and it is equal to the weighted sum of the neighboring stacked traces. The interpolation weights are functions of the distance between the midpoint location of the model trace and the midpoint location of the data trace. The sum of all the weights corresponding to one data trace is usually equal to one. Because the weights are independent from time along the seismic traces, for sake of notation simplicity, we collapse the time axis and consider each element d_i of the data space (recorded data) $\mathbf{d}$, and each element m_j of the model space $\mathbf{m}$ (stacked volume), as representing a whole trace. The relationship between data and model is linear and can be expressed as,

$$d_i = \Sigma_j \, a_{ij} \, m_j; \text{ subject to the constraint } \Sigma_j \, a_{ij} = 1. \tag{1}$$

In matrix notation, equation (1) becomes

$$\mathbf{d} = \mathbf{A}\mathbf{m}. \tag{2}$$

where the model vector $\mathbf{m}$ is the composite of all the offset/azimuth cubes $\mathbf{m_h}$, that is

$$\mathbf{m} = \begin{bmatrix} \mathbf{m}_{\mathbf{h}_1} \\ \vdots \\ \mathbf{m}_{\mathbf{h}_i} \\ \vdots \\ \mathbf{m}_{\mathbf{h}_n} \end{bmatrix}. \tag{3}$$

Stacking is the summing of the data traces into the model traces weighted by the interpolation weights. In operator notation, stacking can be represented as the application of the adjoint

operator $\mathbf{A}'$ to the data traces (Claerbout, 1998); that is,

$$\mathbf{m} = \mathbf{A}'\mathbf{d}. \tag{4}$$

The application of simple stacking as an adjoint operator does not yield satisfactory results when the fold is unevenly distributed among midpoint bins. In the stack, the amplitudes of the bins with higher fold will be artificially higher than the amplitudes of the bins with lower fold. To compensate for this uneveness in the fold, it is common practice to divide the stacked traces by the inverse of the fold. This fold normalization can be also expressed in operator notation when a diagonal operator $\mathbf{W}_m$ is added in front of the adjoint operator in the computation of the stack:

$$\mathbf{m} = \mathbf{W}_m\mathbf{A}'\mathbf{d} = \mathbf{d}. \tag{5}$$

The weights w_j^m are given by the inverse of the fold, that can be simply computed by a summation of the elements in each column of $\mathbf{A}$; that is,

$$w_j^m = \left(\Sigma_i\ a_{ij}\right)^{-1}. \tag{6}$$

Data gaps in the fold present a problem for fold normalization because they make the weights diverge to infinity in equation (6). To avoid instability, it is common practice to add a small number ϵ_w to the actual fold, or to set the weights to zero when the fold is smaller than ϵ_w, as in the following revised expression for the weights:

$$w_j^m = \begin{cases} \left(\Sigma_i\ a_{ij}\right)^{-1} & \text{if } \Sigma_i\ a_{ij} \geq \epsilon_w \\ \\ 0 & \text{elsewhere.} \end{cases} \tag{7}$$

We derived the fold normalization by a simple heuristic, and it may seem an *ad hoc* solution to the problem of normalizing the output of stacking. However, it can be shown that the weights used by fold normalization can be derived from applying the general theory of inverse least-squares to the stacking normalization problem (Biondi, 1999). The least-squares problem is

$$0 \approx \mathbf{d} - \mathbf{A}\mathbf{m}, \tag{8}$$

and its formal solution can be written as

$$\mathbf{m} = \mathbf{A}^{\ddagger}{}_m\mathbf{d} = \left(\mathbf{A}'\mathbf{A}\right)^{-1}\mathbf{A}'\mathbf{d}. \tag{9}$$

where the operator $\mathbf{A}^{\ddagger}{}_m$ is often referred as the pseudoinverse (Strang, 1986). Applying the least-squares inverse is equivalent to applying the adjoint operator $\mathbf{A}'$ followed by a *spatial filtering* of the model space given by the inverse of $\mathbf{A}'\mathbf{A}$. The fold normalization can be seen as a particular approximation of the inverse of $\mathbf{A}'\mathbf{A}$ with a diagonal operator. Because of the size of the problem, computing the exact inverse of $\mathbf{A}'\mathbf{A}$ is not straightforward. We have thus two choices: 1) to compute an analytical approximation to the inverse; 2) to use an iterative method to compute a numerical approximation to the inverse. Even if we follow the second strategy, the availability of an analytical approximation to the inverse is useful, because the approximate inverse can be used as a preconditioner to accelerate the convergence of the iterative inversion.

We will discuss two methods for approximating the inverse of $\mathbf{A}'\mathbf{A}$. The first method is algebraic and it is based on the direct manipulation of the elements of $\mathbf{A}'\mathbf{A}$, such as extracting its diagonal or summing the elements in its columns (or rows). The second method is based on the idea that for capturing the most significant properties of $\mathbf{A}'\mathbf{A}$ by measuring its effects when applied to a reference model ($\mathbf{m}_{\text{ref}}$) (Claerbout and Nichols, 1994; Rickett, 2001).

Although these two methods seems unrelated, they yield equivalent results for specific choices of $\mathbf{m}_{\text{ref}}$. Therefore, the second method can be used to analyze the assumptions that underly the possible choices of approximations.

Approximation of $\mathbf{A}'\mathbf{A}$ by the sum of its columns

We now analyze the properties of the approximate inverse that is defined by the substitution of $\mathbf{A}'\mathbf{A}$ with a diagonal matrix $\widetilde{\mathbf{A}'\mathbf{A}}$, when the diagonal elements of $\widetilde{\mathbf{A}'\mathbf{A}}$ are equal to the sum of the corresponding rows of $\mathbf{A}'\mathbf{A}$. Notice that $\mathbf{A}'\mathbf{A}$ is symmetric, and thus summing over the columns would be equivalent to summing over the rows. It can be noticed that the diagonal elements of $\widetilde{\mathbf{A}'\mathbf{A}}$ are equal to the sum of the columns of the original operator $\mathbf{A}$ as defined in equation (1); i.e., they are equal to the fold computed for each corresponding model trace. The weights a_{lj} are interpolator weights, and they fulfill the constraint $\Sigma_j\ a_{lj} = 1$ expressed in equation (1). It immediately follows that

$$^{\Sigma}w_i^m = (\Sigma_l\ \ a_{li})^{-1}, \tag{10}$$

which is equivalent to equation (6). In summary, we just derived, for the model-space inverse, an approximation that is easy to compute, and it is equal to the fold normalization that was defined by heuristic considerations. However, the definition of the approximate inverse can be applied when more complex imaging operators are involved, and for which we do not have a simple heuristic to define the weights that improve the results obtained by application of the adjoint operator.

Approximation of $\mathbf{A}'\mathbf{A}$ by application to a reference model ($\mathbf{m}_{\text{ref}}$)

The second method is based on the idea that for capturing the most significant properties of $\mathbf{A}'\mathbf{A}$ by measuring its effects when applied to a reference model ($\mathbf{m}_{\text{ref}}$).

The approximation is then evaluated as

$$\mathbf{A}'\mathbf{A} \approx \frac{\mathbf{diag}\left(\mathbf{A}'\mathbf{A}\,\mathbf{m}_{\text{ref}}\right)}{\mathbf{diag}\,(\mathbf{m}_{\text{ref}})}. \tag{11}$$

This method has the important advantage that it does not require the explicit evaluation (and storage) of the elements of $\mathbf{A}'\mathbf{A}$, but it just requires its application to a reference model. Of course, the resulting approximation is strongly dependent from the choice of the reference model. The closer is the reference model to the true model, the better is the approximation. In theory, if the reference model is equal to the true model we will achieve perfect results.

It is also easy to show that the approximation of $\mathbf{A}'\mathbf{A}$ by the sum of its columns, equation (10), is equivalent to the choice of a constant vector as $\mathbf{m}_{\text{ref}}$ in equation (11). Therefore, it will bias the imaging process towards model that are constant. In the case of stacking, it encourages flat reflectors, that is consistent with the flat reflector assumptions underlying the stacking process. In the case of a more complex imaging operator aimed at imaging complex structure, this bias towards flat reflectors may be less appropriate.

Fold normalization is effective when the geometry is irregular but without sizable data gaps. However, when these gaps are present the normalization weights tend to become large. Even if instability can be easily avoided by the weights modification expressed in equation (7), gaps are going to be left in the uniformly sampled data. These gaps are likely to introduce artifacts in the image because migration operators spread them as *migration smiles*. The gaps should be filled using the information from nearby traces before migration. In the next section we discuss how that can be done within the context of inverse theory.

MODEL REGULARIZATION AND PRECONDITIONING

In the previous section we have seen that data gaps are a challenge for simple fold normalization. To fill the gaps, we want to use the information from traces recorded with geometry similar to the missing ones. The challenge is to devise a method that maximizes the image resolution and minimizes artifacts.

Given no *a priori* knowledge on the reflectors geometry, using the information from traces from the surrounding midpoints and same offset-azimuth range can cause a resolution loss because it may smooth true reflectivity changes. On the other hand, because of physical constraints on the reflection mechanism, the reflection amplitudes can be assumed to be a smooth function of the reflection angle and azimuth. This observation leads to the idea that smoothing the data over offset and azimuth could be performed without losing resolution. Ideally, such smoothing should be done over aperture angles (dip and azimuth) at the reflection location, not over offset and azimuth at the surface. However, smoothing at the reflectors would require a full migration of the data. The migration step would make the method dependent on the accurate knowledge of the interval velocity model. This reliance on the velocity model is inescapable when the imaging problems are caused by the complexities in velocity model itself, (e.g. subsalt illumination (Prucha et al., 2001)), but it ought to be avoided when the imaging problems are caused by irregularities in the acquisition geometries.

In the context of least-squares inversion, smoothing along offset/azimuth in the model space (e.g. uniformly sampled offset/azimuth cubes) can be accomplished by introducing a model regularization term that penalizes variations of the seismic traces between the cubes. The simple least-squares problem of equation (8) then becomes

$$\begin{aligned} 0 &\approx \mathbf{d} - \mathbf{A}\mathbf{m} \\ 0 &\approx \epsilon_D \mathbf{D}_{\mathbf{h}}' \mathbf{D}_{\mathbf{h}} \mathbf{m}, \end{aligned} \tag{12}$$

where the *roughener* operator $\mathbf{D_h}$ is

$$\mathbf{D_h} = \frac{1}{1-\rho_D} \begin{bmatrix} 1-\rho_D\mathbf{I} & 0 & 0 & \vdots & 0 & 0 \\ -\rho_D\mathbf{I} & \mathbf{I} & 0 & \vdots & 0 & 0 \\ 0 & -\rho_D\mathbf{I} & \mathbf{I} & \vdots & 0 & 0 \\ ... & ... & \ddots & \vdots & 0 & 0 \\ 0 & 0 & ... & \ddots & -\rho_D\mathbf{I} & \mathbf{I} \end{bmatrix}. \tag{13}$$

The coefficient ρ_D must be between 0 and 1. It determines the range over which we smooth the offset/azimuth cubes. Smaller the value we set for ρ_D, narrower the smoothing range is.

Regularization with a roughener operator such as $\mathbf{D_h^{'}D_h}$ has the computational drawback that it substantially worsens the conditioning of the problem, making the solution more expensive. However, the problem is easy to precondition because $\mathbf{D_h^{'}D_h}$ is easy to invert, since it is already factored in a lower block-diagonal operator $\mathbf{D_h}$ and in an upper block-diagonal operator $\mathbf{D_h^{'}}$, that can be inverted by recursion. Therefore, we can write the preconditioned least-squares problem

$$\begin{aligned} 0 &\approx \mathbf{d} - \mathbf{A}\left(\mathbf{D_h^{'}D_h}\right)^{-1}\mathbf{p} \\ 0 &\approx \epsilon_D\mathbf{I}\mathbf{p}, \end{aligned} \tag{14}$$

where $\mathbf{p} = \mathbf{D_h^{'}D_h m}$ is the preconditioned model vector.

To take into account fold variations we can introduce a diagonal scaling factor, by applying the same theory discussed in the previous section. The weights for the regularized and preconditioned problem are thus computed as

$$\mathbf{W_I^{-1}} = \frac{\mathbf{diag}\left\{\left[\left(\mathbf{D_h D_h^{'}}\right)^{-1}\mathbf{A^{'}A}\left(\mathbf{D_h^{'}D_h}\right)^{-1} + \epsilon_D\mathbf{I}\right]\mathbf{p}_{\text{ref}}\right\}}{\mathbf{diag}\left(\mathbf{p}_{\text{ref}}\right)}. \tag{15}$$

Notice that because of the nature of $\mathbf{D_h^{'}D_h}$, $\mathbf{p}_{\text{ref}} = \mathbf{D_h^{'}D_h m}_{\text{ref}} = \mathbf{D_h^{'}D_h 1} = \mathbf{1}$, and $\left(\mathbf{D_h^{'}D_h}\right)^{-1}\mathbf{1} = \mathbf{1}$, and some computation can be saved by computing the weights as

$$\mathbf{W_I^{-1}} = \frac{\mathbf{diag}\left\{\left[\left(\mathbf{D_h D_h^{'}}\right)^{-1}\mathbf{A^{'}A} + \epsilon_D\mathbf{I}\right]\mathbf{1}\right\}}{\mathbf{diag}(\mathbf{1})}. \tag{16}$$

In this case the computational cost of applying twice the leaky integrator $\left(\mathbf{D_h^{'}D_h}\right)^{-1}$ to the model vector is small, thus the computational saving is trivial. However, when we introduce more expensive operators to smooth the data over offset/azimuth, substituting equation (15) with equation (16) halves the computational cost of evaluating the weights. The solution of the problem obtained by normalizing the preconditioned adjoint is

$$\widetilde{\mathbf{m}} = \left(\mathbf{D_h^{'}D_h}\right)^{-1}\mathbf{W_I}\left(\mathbf{D_h D_h^{'}}\right)^{-1}\mathbf{A^{'}d}. \tag{17}$$

The normalization weights could be used for another preconditioning step, by using them in another change of variables $\mathbf{q} = \mathbf{W_I}^{-\frac{1}{2}}\mathbf{p}$. This would yield the following least-squares problem,

$$\begin{aligned} 0 &\approx \mathbf{d} - \mathbf{A}\left(\mathbf{D_h'}\mathbf{D_h}\right)^{-1}\mathbf{W_I}^{\frac{1}{2}}\mathbf{q} \\ 0 &\approx \epsilon_D \mathbf{I}\mathbf{W_I}^{\frac{1}{2}}\mathbf{q}. \end{aligned} \tag{18}$$

If the problem expressed in equations (18) were to be solved iteratively, it is likely that it would converge faster than either the original regularized problem [equations (12)] or the preconditioned problem [equations (14)]. However, we prefer a non-iterative solution both because it is cheaper, and because it is somewhat more predictable.

Regularization by AMO

The main drawback of the method described above is that smoothing over offset/azimuth cubes by the inverse of the simple roughener operator expressed in equation (13) may result in loss of resolution when geological dips are present. It is well know that dipping events are not flattened by NMO with the same velocity as flat events. However, the method is easily generalized by substitution of the identity matrix in the lower diagonal of $\mathbf{D_h}$ with an appropriate operator that correctly transforms a common offset-azimuth cube into an equivalent cube with a different offset and azimuth. This can be accomplished by AMO (Biondi et al., 1998). Since the cubes to be transformed are uniformly sampled we can use a Fourier-domain formulation of AMO that is both efficient and straightforward to implement (Vlad and Biondi, 2001). The roughener operator that includes AMO is then expressed as

$$\widetilde{\mathbf{D}}_\mathbf{h} = \frac{1}{1-\rho_D}\begin{bmatrix} 1-\rho_D\mathbf{I} & 0 & 0 & \vdots & 0 & 0 \\ -\rho_D\mathbf{T}_{\mathbf{h}_{1,2}} & \mathbf{I} & 0 & \vdots & 0 & 0 \\ 0 & -\rho_D\mathbf{T}_{\mathbf{h}_{2,3}} & \mathbf{I} & \vdots & 0 & 0 \\ ... & ... & \ddots & \vdots & 0 & 0 \\ 0 & 0 & ... & \ddots & -\rho_D\mathbf{T}_{\mathbf{h}_{n-1,n}} & \mathbf{I} \end{bmatrix}, \tag{19}$$

where $\mathbf{T}_{\mathbf{h}_{i,i+1}}$ is the AMO operator that transforms the offset-azimuth cube i into the offset-azimuth cube $i+1$. The $\widetilde{\mathbf{D}}_\mathbf{h}'\widetilde{\mathbf{D}}_\mathbf{h}$ operator can also be easily inverted by recursion and thus the least-squares problem obtained by substituting $\widetilde{\mathbf{D}}_\mathbf{h}$ for $\mathbf{D_h}$ in equations (12) can also be easily preconditioned and normalized using the same techniques described in equations (14-18).

IMAGING OF A 3-D LAND DATA SET

We tested the geometry regularization methods presented in the previous section on a land data set recorded in South America. The data were shot with a cross-swath geometry. The shot lines are not perfectly aligned along the perpendicular to the receiver lines, but they are

oriented at an angle (about 18 degrees). Figure 1 shows the plot of the absolute offset vs. azimuth for a random sample of traces in the data set. For land data, the data set has fairly narrow-azimuth acquisition geometry.

Figure 2 shows three sections (depth slice on the top, cross-line section in the middle, and in-line section on the right) of the near-angle stack of the migrated data. At a depth of about 3.2 km there is a producing reservoir with numerous wells that could be used in future work to evaluate the imaging results. The only a structural feature in the data is a steep folding/faulting at the reservoir level. There are subtle stratigraphic features at a shallower depth, such as the channel visible in the upper-left corner of the depth slice in the figure (depth of 1.9 km).

The processing sequence comprised of the following steps: a) NMO, b) geometry regularization, c) inverse NMO, d) 3-D prestack common-azimuth wave-equation migration, with the imaging step designed to preserve relative amplitudes, as discussed by Sava and Biondi (2001). The velocity model was fairly simple. The NMO velocity was slightly varying in the lateral direction. However, we migrated the data using an interval velocity only as a function of depth.

To test the relative performances of the different geometry regularization methods we migrated the data after regularizing the geometries with three different methods: a) normalization by partial stack fold [equation (5)]; we will simply call this method *normalization*. b) normalization of the regularized and preconditioned solution without AMO [equation (17)]; we will simply call this method *regularization*, c) normalization of the regularized and preconditioned solution with AMO [equation (17) with $\mathbf{D_h} = \widetilde{\mathbf{D}}_\mathbf{h}$, as in equation (19)]; we will call this method *AMO regularization*.

The geometry regularizations produced common offset/azimuth cubes at zero azimuth and with offset sampling of 195 m, in-line midpoint sampling of 25 m, and cross-line midpoint sampling of 50 m. By assuming reciprocity, the offset sign was ignored to increase the effective fold of the common offset/azimuth cubes. Our first tests to regularize the data geometry produced common offset-azimuth cubes at zero azimuth (i.e. the data azimuth was ignored) because of the fairly limited azimuthal range at far offsets. However, we have indications that taking into account the data azimuth for the far-offset traces may be beneficial.

The offset axis was resampled at 65 m by simple interpolation before migration, to avoid offset aliasing in the downward continuation. This offset sampling was selected to avoid aliasing artifacts at the reservoir level. Finer sampling would be necessary to migrate shallower events without aliasing the higher frequencies present in the seismic signal. The effects of irregular geometries are more evident at shallow depth, and interesting stratigraphic features are visible in the migrated stack as shallow as 1 km depth. Therefore, future tests may be directed to produce high-quality images shallower than the tests that we present in this paper.

Geometry regularization results

Figure 3 compares the results of geometry regularization of the three methods discussed above for one line. Figure 3a shows the results for normalization, Figure 3b shows the results for

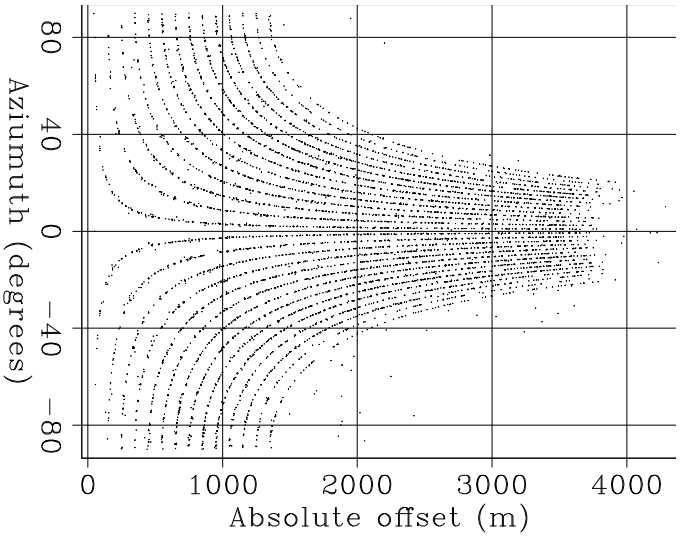

Figure 1: Offset-azimuth distribution of the land data set from South America. biondo1-OffAz [CR]

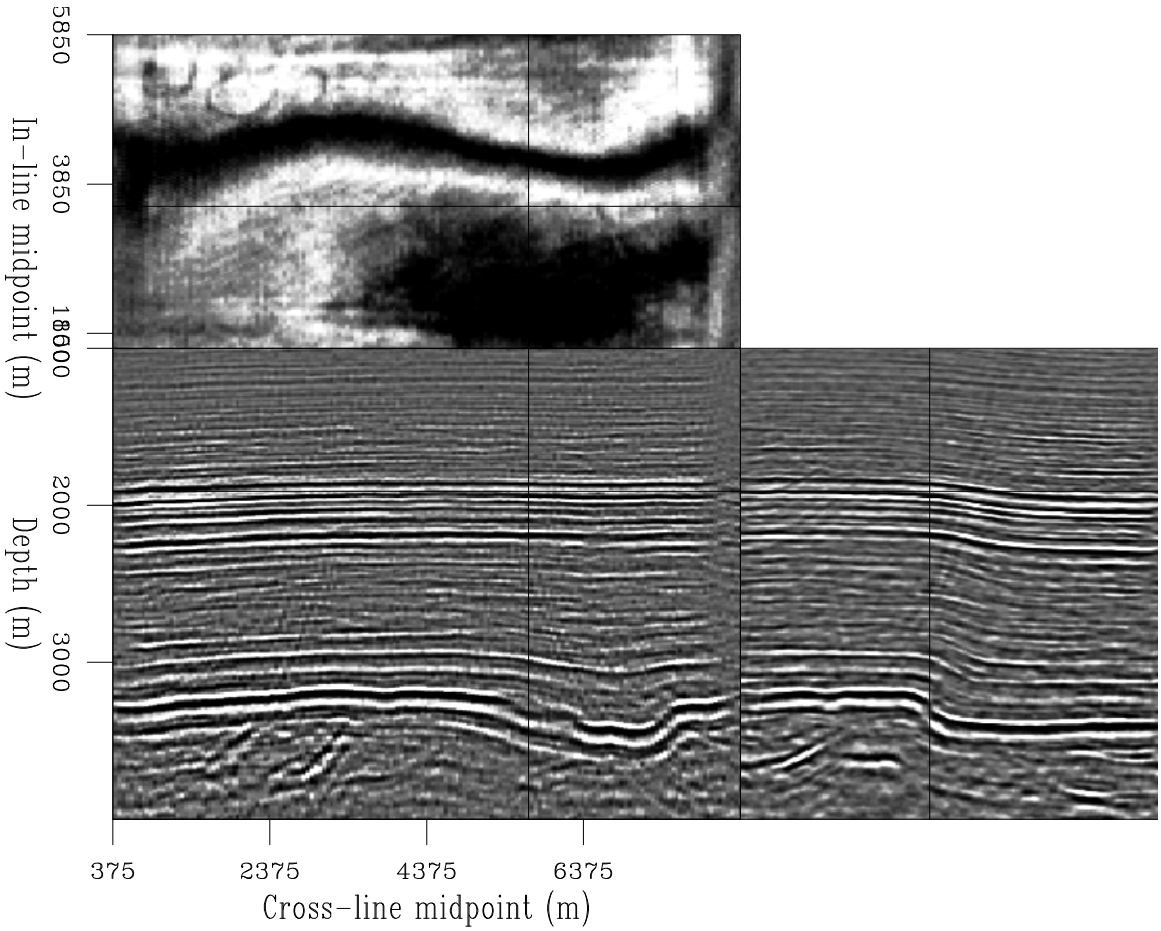

Figure 2: Near-angle stack of the migrated cube. biondo1-Wm_lin_all_reg_vz_mig_nang_stack [CR]

regularization, and Figure 3c shows the results for AMO regularization. Comparing the in-line sections at one offset (3.38 km) shows the advantages of both regularization and AMO regularization over simple normalization. The data amplitudes after normalization are still fairly uneven, and thus they are likely to produce artifacts during the migration. On the contrary, in the data obtained using regularization the data amplitudes are better balanced. The steeply dipping reflection from the fold at the reservoir level is better preserved in the AMO regularization results than in the simple regularization results. The reason is quite apparent when examining the data as a function of offset for one particular midpoint location. The dipping event is smiling upward after NMO, and thus it is attenuated by simple smoothing over offset.

Figure 4 shows a detail of the same line that illustrates the effects of the regularization term during the process. As for Figure 3, Figure 4a shows the results for normalization, Figure 4b shows the results for regularization, and Figure 4c shows the results for AMO regularization. An acquisition gap is clearly visible in the middle of the constant-offset (2.275 km) section in panel (a). Simple normalization cannot fill the gap. On the contrary, the gap is filled in the regularized results, that exploit the information from the neighboring offsets. The gap in the dipping event is better filled by the AMO regularization because the information from neighboring offsets is moved to the missing data consistently with their kinematics. The differences in behavior between the two regularization methods are apparent when analyzing the time slices in the upper part of the figure. As the dipping event moves towards higher offset (up), it also moves towards further midpoint (right). This movement is well seconded by the AMO regularization, while it is smoothed over by the simpler regularization scheme.

Amplitude-preserving migration results

We migrated the data after geometry regularization using common-azimuth migration and produced three different prestack migrated images with the Common Image Gathers (CIG) function of the in-line offset ray parameter (p_{hx}). Figure 5 compares one line extracted at CMPY=5.775 km, for a wide reflection angle. As before, panel (a) displays the result obtained using normalization, panel (b) displays the result obtained using regularization, and panel (c) displays the result obtained using AMO regularization. The image obtained by normalization is more noisy than the ones obtained by using regularization. The fold is slightly better imaged in the results using AMO regularization (panel c). These differences are confirmed in the depth slices shown in Figure 6 shows two depth slices taken at the reservoir level (depth 3.27 km) obtained by migration after geometry regularization with: normalization (top), regularization (middle) AMO regularization (bottom). Panels (a) show the images for a narrow reflection angle, panels (b) show the images for a wide reflection angle. The depth slices obtained using normalization are noisier than the ones obtained using regularization. The dipping event (marked as Fold in the figures) is better imaged in both the normalization results and in the AMO regularization results than in the regularization results.

There are also other subtle differences between the two images obtained with regularization. Only a joint analysis of the seismic images with the well logs from the existing well could determine if they are significant for the accuracy of reservoir characterization.

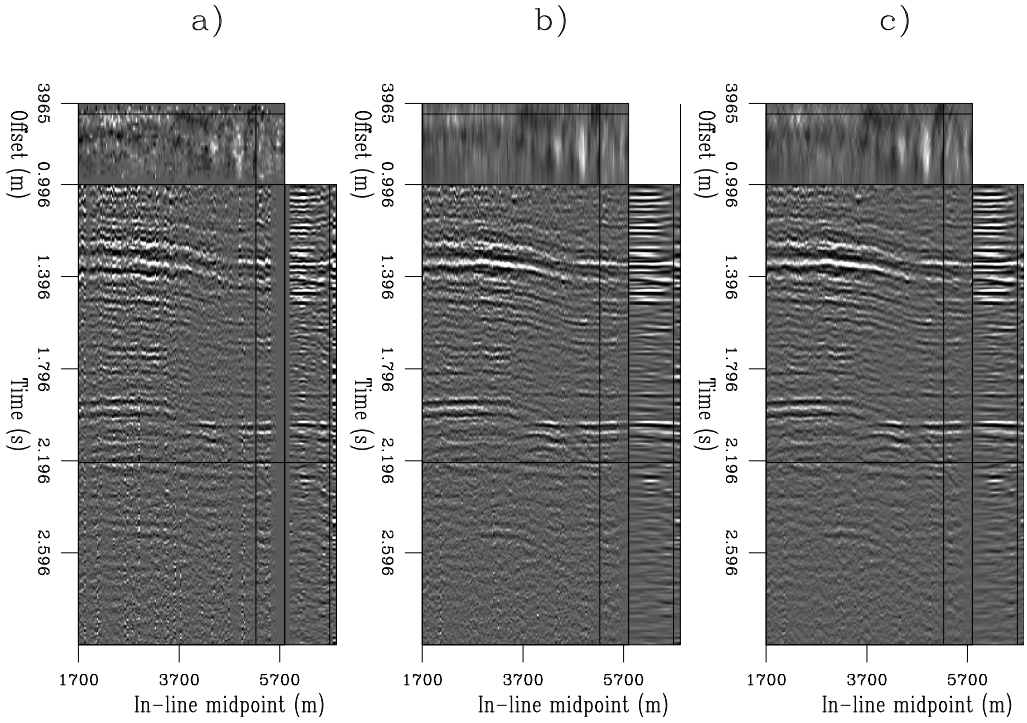

Figure 3: A prestack line after geometry regularization with: a) normalization, b) regularization, c) AMO regularization. biondo1-Data_abc [CR]

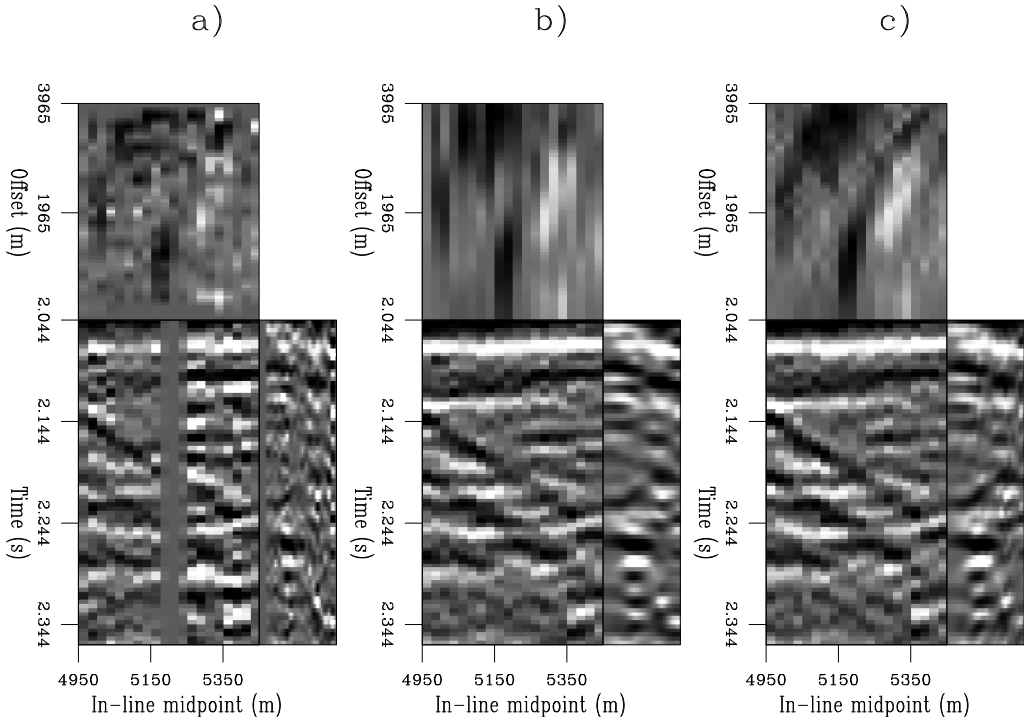

Figure 4: A detail of the prestack line shown in Figure 3. Notice the data gap in the middle of the common-offset (2.275 km) section, and how it has been interpolated differently by regularization (panel b) and AMO regularization (panel c). biondo1-Data_win_abc [CR]

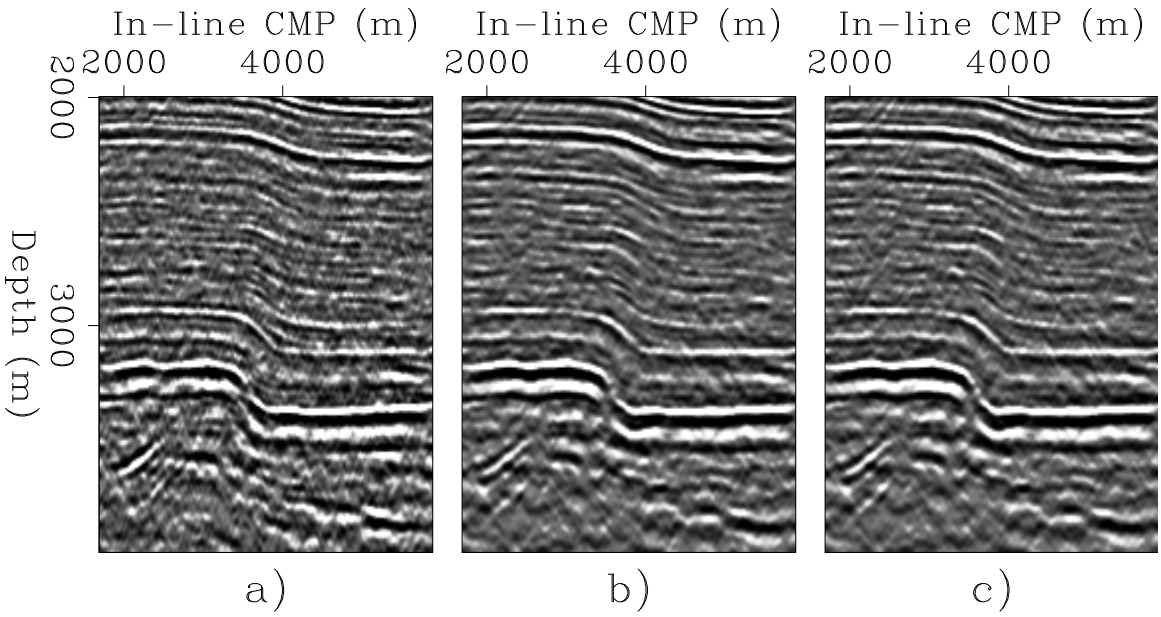

Figure 5: Images for wide reflection angle at constant cross-line location (CMPY=5.775 km). The images were obtained after geometry regularization with: a) normalization, b) regularization, c) AMO regularization. biondo1-Line_abc [CR]

Figure 7 shifts our attention to a shallower level, where there are no obvious structural features, but meandering channels are visible. The depth slices were taken at a depth of 1.91 km. One channel is clearly visible in the upper left corner of the images, while another one is (less clearly) visible around the lower right corner of the images. As for the previous figures, the slices on the left are taken for a narrow reflection angle, the slices on the right are taken for a wide reflection angle. The images obtained using normalization are noisier and show more clearly the oblique acquisition footprints. In the narrow angle image, the noise is so overwhelming that no channels are visible. The two regularization results are comparable for narrow angles. At wider angle the AMO regularization image is slightly better focused. Subtle differences are noticeable in the imaging of both channels, where indicated by the arrows. Although the images of the upper channel are unfortunately affected by edge effects caused by the migration.

CONCLUSIONS

The proposed method for regularizing the geometry of 3-D prestack data set performed well in a real-data test. The analysis of the data after geometry regularization demonstrates that the regularization methods fill the acquisition gaps by using the information from neighboring offsets/azimuths. Therefore, they provide a better input to the migration than the simple normalization by the partial stack fold. The imaging results confirm this analysis.

The inclusion of the AMO operator in the regularization assures better preservation of the

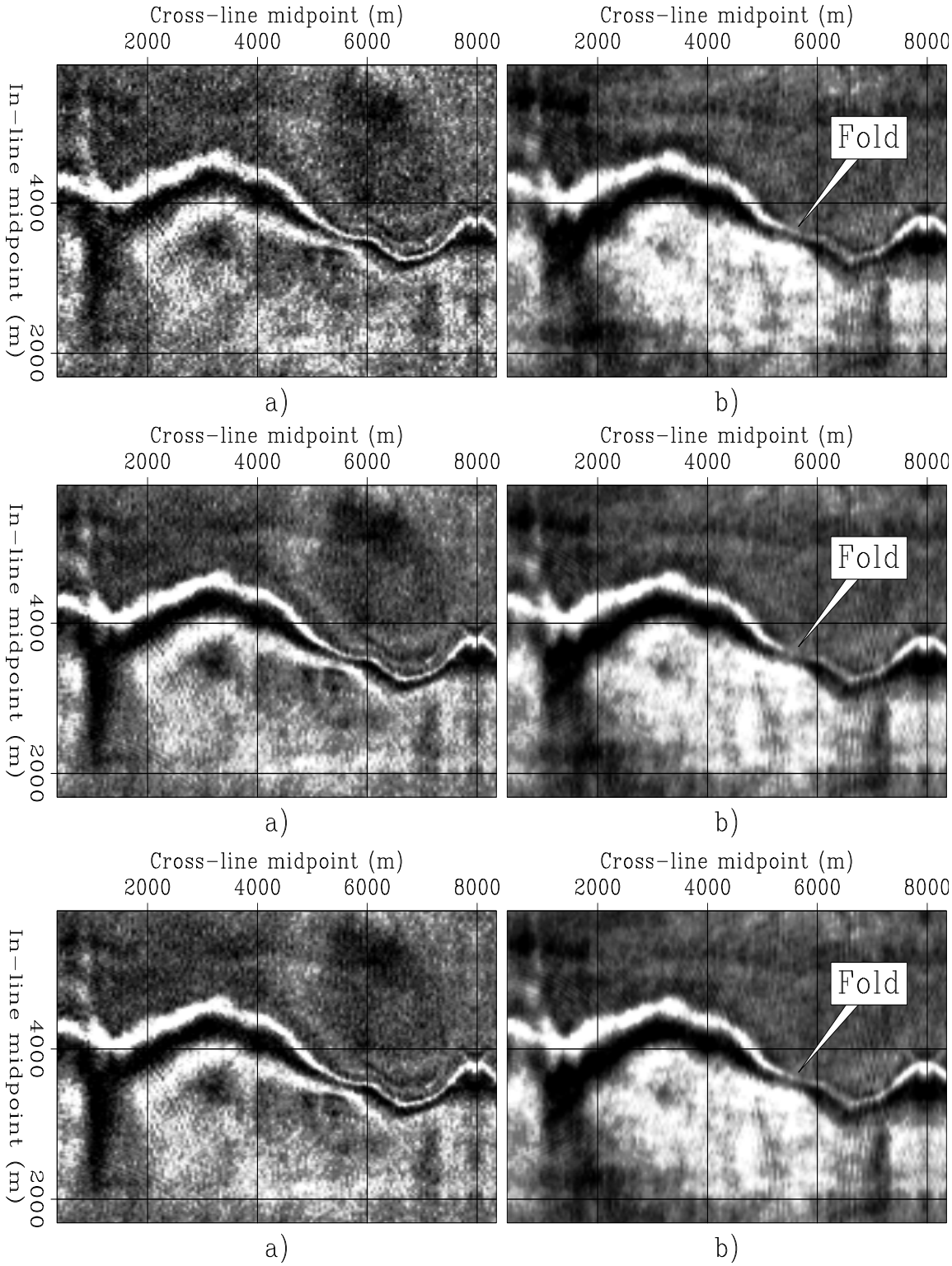

Figure 6: Depth slices, at a depth of 3.27 km, obtained by migration after geometry regularization with: normalization (top), regularization (middle) AMO regularization (bottom). Narrow reflection angle (left), and wide reflection angle (right). biondo1-3270 [CR]

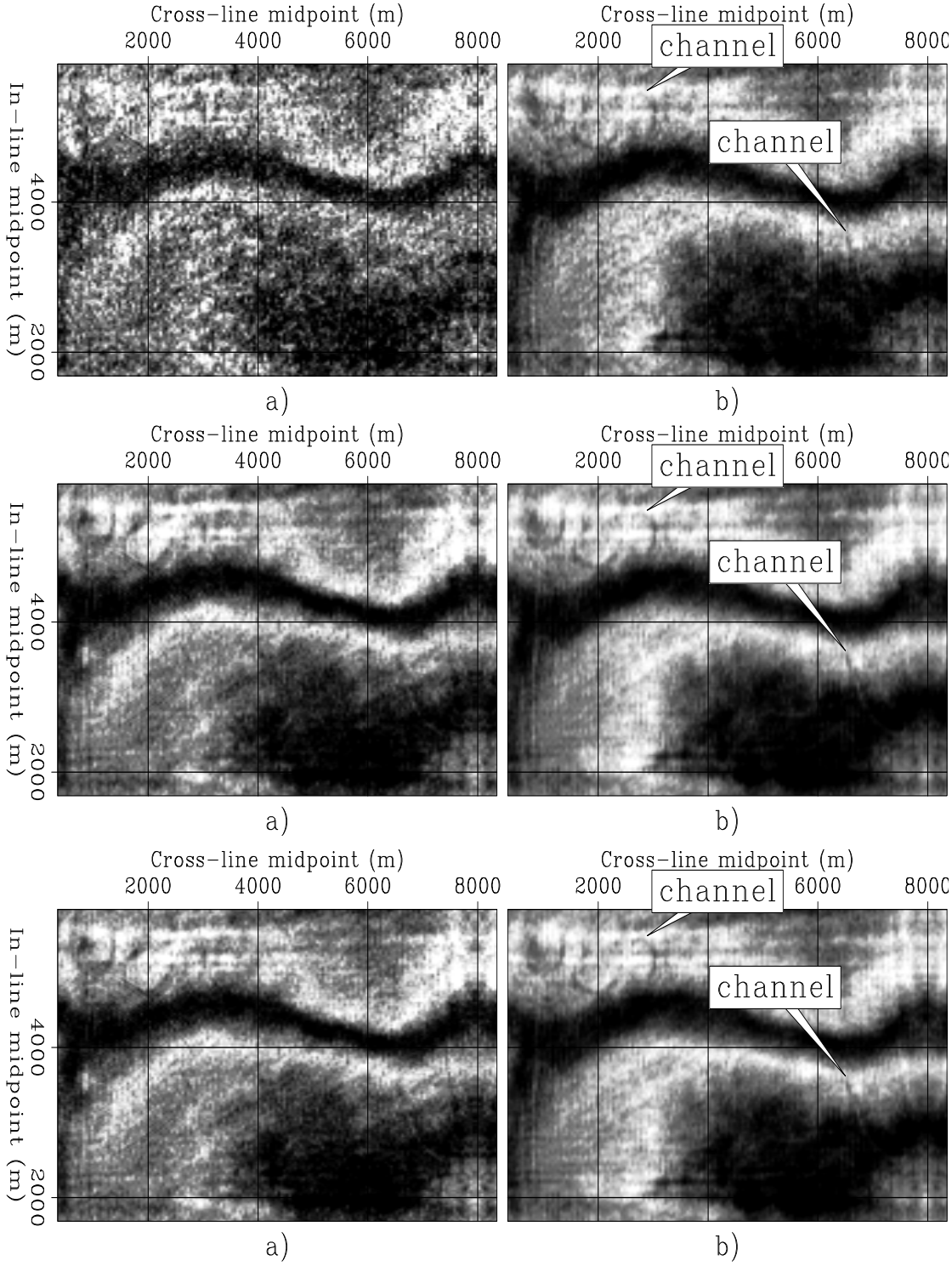

Figure 7: Depth slices, at a depth of 1.91 km, obtained by migration after geometry regularization with: normalization (top), regularization (middle) AMO regularization (bottom). Narrow reflection angle (left), and wide reflection angle (right). biondo1-1910 [CR]

steeply dipping event, thus yielding higher-resolution images than when the AMO operator is not applied. At the reservoir level (depth of 3.2 km), the improvements in the images are fairly subtle. We would expect more substantial differences for shallower events. However, the processing parameters (in particular, offset sampling for migration) were not optimized for shallow targets. Furthermore, in the tests presented in these paper we ignored the data azimuth. Preliminary tests indicated that taking into account the data azimuth when regularizing the geometry can improve the results at far offset. The method and the codes are ready for these further tests.

An obvious improvement to the method is to allow the the smoothing range parameter (ρ_D) to vary. A non-stationary regularization could better take into account the local sparseness in the data. Using ρ_D that changes laterally could be dangerous and lead to instability, but making it function of depth should be trivial and makes sense because the smoothing range ought to be constant as a function of the reflection angle at depth, not of the offset at the surface.

ACKNOWLEDGMENTS

We would like to thank Trino Salinas from Ecopetrol for bringing the data set to SEP during his visit this summer, and Ecopetrol for making the data available to SEP.

REFERENCES

Albertin, U., Jaramillo, H., Yingst, D., Bloor, R., Chang, W., Beasley, C., and Mobley, E., 1999, Aspects of true amplitude migration: 69th Annual Internat. Mtg., Soc. Expl. Geophys., Expanded Abstracts, 1358–1361.

Audebert, F., 2000, Restored amplitudes AVA-gathers in the multi-angle domain: 62nd Mtg. Eur. Assoc. Expl Geophys., Abstracts, P–142.

Biondi, B., Fomel, S., and Chemingui, N., 1998, Azimuth moveout for 3-D prestack imaging: Geophysics, **63**, no. 2, 574–588.

Biondi, B. L., 1999, 3-D Seismic Imaging: `http://sepwww.stanford.edu/sep/biondo/Lectures/index.html`.

Bloor, R., Albertin, U., Jaramillo, H., and Yingst, D., 1999, Equalised prestack depth migration: 69th Annual Internat. Mtg., Soc. Expl. Geophys., Expanded Abstracts, 1358–1361.

Chemingui, N., and Biondi, B., 1997, Equalization of irregular data by iterative inversion: Expanded Abstracts, 1115–1118.

Chemingui, N., 1999, Imaging irregularly sampled 3D prestacked data: SEP–**101**.

Claerbout, J., and Nichols, D., 1994, Spectral preconditioning: SEP–**82**, 183–186.

Claerbout, J., 1998, Geophysical estimation by example: Environmental soundings image enhancement: http://sepwww.stanford.edu/sep/prof/.

Duijndam, A. J. W., Volker, A. W. F., and Zwartjes, P. M., 2000, Reconstruction as efficient alternative for least squares migration: 70th Ann. Internat. Meeting, Soc. Expl. Geophys., Expanded Abstracts, to be published.

Duquet, B., Marfurt, K., and Dellinger, J., 1998, Efficient estimates of subsurface illumination for Kirchhoff prestack depth migration: 68th Ann. Internat. Meeting, Soc. Expl. Geophys., Expanded Abstracts, 1541–1544.

Fomel, S., 2001, Three-dimensional seismic data regularization: Ph.D. thesis, Stanford University.

Nemeth, T., Wu, C., and Schuster, G. T., 1999, Least-squares migration of incomplete reflection data: Geophysics, **64**, no. 1, 208–221.

Prucha, M. L., Clapp, R. G., and Biondi, B. L., 2001, Imaging under salt edges: A regularized least-squares inversion scheme: SEP–**108**, 91–104.

Rickett, J., 2001, Model-space vs data-space normalization for finite-frequency depth migration: SEP–**108**, 81–90.

Ronen, S., 1987, Wave-equation trace interpolation: Geophysics, **52**, no. 7, 973–984.

Rousseau, V., Nicoletis, L., Svay-Lucas, J., and Rakotoarisoa, H., 2000, 3D true amplitude migration by regularisation in angle domain: 62nd Mtg. Eur. Assoc. Expl Geophys., Abstracts, B–13.

Sava, P., and Biondi, B., 2001, Amplitude-preserved wave-equation migration: SEP–**108**, 1–26.

Strang, G., 1986, Linear Algebra and its Applications: Harcourt Brace Jovanovich College Publishers.

Vlad, I., and Biondi, B., 2001, Effective AMO implementation in the log-stretch, frequency-wavenumber domain: SEP–**110**, 63–70.